Modelling and Dynamic Behaviour of Variable Speed Wind Turbines Using Doubly Fed Induction Generators (DFIG)

By
Ram Mohana Vamsee.B, Prof. D.S.Bankar, Dr. D. B. Talange,

Abstract : **- Doubly fed induction generator (DFIG) finds the wide application in wind power generation system due to its superb quality of controlling active and reactive power independently and partial power converter.**

This paper presents the dynamic behaviour of a wind turbine equipped with a doubly fed induction generator (DFIG) in case of disturbances in the interconnected grid. A model of a DFIG is presented and adapted for analysing the response of the wind generator to voltage control, frequency control, voltage sags and wind variations. The rotor-side converter (RSC) and grid-side converter (GSC) of the DFIG are controlled in a (d-q) reference frame. The transient performance of DFIG wind turbines is evaluated under super-synchronous and sub-synchronous operation during different grid voltage dips. Details of the control strategy and system simulation results in Simulink are presented to show the effectiveness of the proposed control strategy.

Index Terms— **Modeling, Wind power generation, Doubly Fed Induction Generator (DFIG), vector control, converter.**

NOMENCLATURE

V_{qs} - q-axis stator voltage,V
V_{ds} - d-axis rotor voltage,V
V_{qr} - q-axis rotor voltage,V
V_{dr} - q-axis rotor voltage,V
I_{qs} - q-axis stator current, A
I_{ds} - d-axis rotor current, A
I_{qr} - q-axis rotor current, A
I_{dr} - q-axis rotor current, A
λ_{ds} - d-axis stator flux linkage, Wb/m2
λ_{qs} - q-axis stator flux linkage,Wb/m2
λ_{qr} - q-axis rotor flux linkage,Wb/m2
λ_{dr} - d-axis rotor flux linkage,Wb/m2
R_s - stator resistance, Ω
R_r - rotor resistance, Ω
ω_s - angular speed of the synchronously rotating reference frame, rad/s
ω_r - Rotational speed of rotor, rad/s
s - Rotor slip

I. INTRODUCTION

Worldwide concern about the environmental pollution and a possible energy crisis has led to increasing interest in technologies for generation of clean and renewable electrical energy. Among various renewable energy sources, wind power is the most rapidly growing one. During the last decade, the concept of a variable-speed wind turbine equipped with a doubly fed induction generator (DFIG) has received increasing attention due to its noticeable advantages over other wind turbine generator (WTG) concepts. In the DFIG concept, the induction generator is grid-connected at the stator terminals, but the rotor terminals are connected to the grid via a partial-load variable frequency AC/DC/AC converter (VFC). The VFC only needs to handle a fraction (25-30%) of the total power to achieve full control of the generator [2] [11] [14].

Much research effort has gone into modelling the DFIG wind turbines and studying their impact on the dynamic performance of the power system. In these works, the power electronic converter models are simplified as controlled ideal voltage-sources or current-sources. This permits large integration time-steps during transient simulations, which is essential in the representation of large networks.

However, in the DFIG WT system, the VFC and its power electronics (IGBT-switches) are the most sensitive part to grid disturbances. The converter action might determine the operation of the WTG during the transient disturbances in the power grid. [1] [9] [10] [12]

II. WIND TURBINE AND DFIG MODEL

The basic configuration of a DFIG wind turbine is shown in Fig. 1. The wound-rotor induction generator in this configuration is fed from both stator and rotor sides. The stator is directly connected to the grid while the rotor is fed through a VFC. In order to produce electrical power at constant voltage and frequency to the utility grid over a wide operating range from subsynchronous to supersynchronous speeds, the power flow between the rotor circuit and the grid must be controlled both in magnitude and in direction. [7].

The operation of the DFIG wind turbine is regulated by a control system, which generally consists of two parts: the electrical control of the DFIG and the mechanical control of the wind turbine blade pitch angle. Control of the DFIG is achieved by controlling the VFC, which includes control of the RSC and control of the GSC, as shown in Fig. 1. [7] [8].

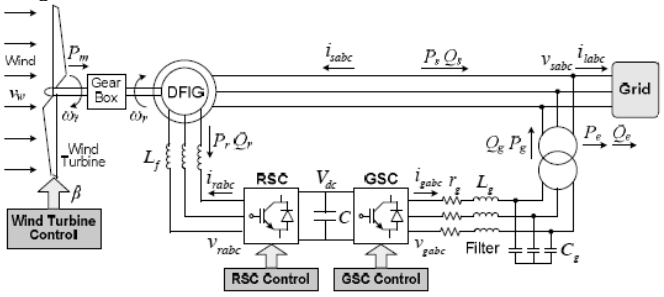

Figure 1 the basic configuration of a DFIG wind turbine

A) Modelling of the Wind Turbine Aerodynamics

The aerodynamic model of a wind turbine can be characterized by the well-known C_P-λ-β curves. C_P is the power coefficient, which is a function of both tip-speed-ratio λ and the blade pitch angle β. The tip-speed-ratio λ is defined by

$$\lambda = \frac{\omega_t R}{v_w} \quad (1)$$

where R is the blade length in m, ω_t is the wind turbine rotational speed in rad/s, and v_w is the wind speed in m/s, and the numerator (ω_{tR}) represents the blade tip speed in m/s of the wind turbine. The C_P-λ-β curves depend on the blade design and are given by the wind turbine manufacturer.

$$C_P(\beta,\lambda) = \sum_{i=0}^{4}\sum_{j=0}^{4}\alpha_{ij}\beta^i\lambda^j \quad (2)$$

Given the power coefficient C_P, the mechanical power that the wind turbine extracts from the wind is calculated by

$$P_m = \tfrac{1}{2}\rho A_r v_w^3 C_P(\lambda,\beta) \quad (3)$$

Where ρ is the air density in kg/m^3, $Ar = \pi R^2$ is the area in m^2 swept by the rotor blades [3] [4].

B) Modelling of the Shaft System

The shaft system of the WTG can be represented either by a two-mass system or by a single lumped-mass system**.** In the two-mass model, separate masses are used to represent the low-speed turbine and the high-speed generator, and the connecting resilient shaft is modelled as a spring and a damper, as shown in Fig.2. The electromechanical dynamic equations are then given by

$$2H_t p\omega_t = T_m - D_t\omega_t - D_{tg}(\omega_t - \omega_r) - T_{tg} \quad (4)$$

$$2H_g p\omega_r = T_{tg} + D_{tg}(\omega_t - \omega_r) - D_g\omega_r - T_e \quad (5)$$

$$pT_{tg} = K_{tg}(\omega_t - \omega_r) \quad (6)$$

In Fig. 2, N_t/N_g is the gear ratio of the gearbox. As in the shaft system is simply modelled as a single lumped-mass system with the lumped inertia constant H_m, calculated by.

$$H_m = H_t + H_g \quad (7)$$

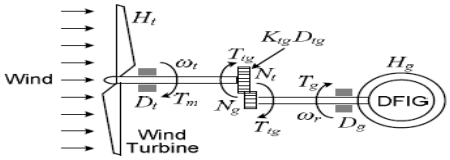

Figure 2. DFIG wind turbine shaft system represented by a two-mass model.[5]

The electromechanical dynamic equation is then given by

$$2H_m p\omega_m = T_m - T_e - D_m\omega_m \quad (8)$$

C) Matlab Simulink Overall Model Of DFIG Connected To Grid

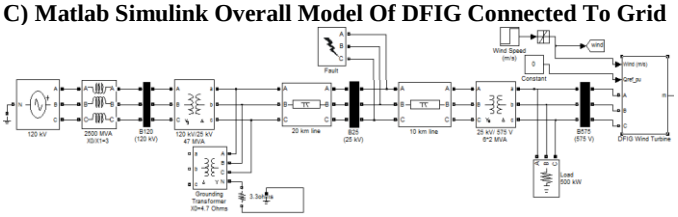

Figure 3 Overall Model of DFIG in Matlab Simulink

A 9 MW wind farm consisting of six 1.5 MW wind turbines connected to a 25 kV distribution system exports power to a 120 kV grid through a 30 km, 25 kV feeder. A 2300V, 2-MVA plant consisting of a motor load (1.68 MW induction motor at 0.93 PF) and of a 200-kW resistive load is connected on the same feeder at bus B_{25}[15].

D) Modelling of the Induction Generator

Taking a single-cage wound rotor induction machine in terms of the instantaneous variables, the stator and rotor equations can be written as

$$v_{sabc} = r_s i_{sabc} + p\lambda_{sabc} \quad (9)$$

$$v_{rabc} = r_r i_{rabc} + p\lambda_{rabc} \quad (10)$$

Applying synchronously rotating reference frame transformation the voltage equations becomes

$$v_{ds} = r_s i_{ds} - \omega_s\lambda_{qs} + p\lambda_{ds} \quad (11)$$

$$v_{qs} = r_s i_{qs} + \omega_s\lambda_{ds} + p\lambda_{qs} \quad (12)$$

$$v_{dr} = r_r i_{dr} - (\omega_s - \omega_r)\lambda_{qr} + p\lambda_{dr} \quad (13)$$

$$v_{qr} = r_r i_{qr} + (\omega_s - \omega_r)\lambda_{dr} + p\lambda_{qr} \quad (14)$$

where ω_s is the rotational speed of the synchronous reference frame, ω_r is the rotor speed, and the flux linkages are given by

$$\lambda_{ds} = L_{ls} i_{ds} + L_m(i_{ds} + i_{dr}) = L_s i_{ds} + L_m i_{dr} \quad (15)$$

$$\lambda_{qs} = L_{ls} i_{qs} + L_m(i_{qs} + i_{qr}) = L_s i_{qs} + L_m i_{qr} \quad (16)$$

$$\lambda_{dr} = L_{lr} i_{dr} + L_m(i_{ds} + i_{dr}) = L_m i_{ds} + L_r i_{dr} \quad (17)$$

$$\lambda_{qr} = L_{lr} i_{qr} + L_m(i_{qs} + i_{qr}) = L_m i_{qs} + L_r i_{qr} \quad (18)$$

where $L_s = L_{ls} + L_m$, $L_r = L_{lr} + L_m$;; L_{ls}, L_{lr} and L_m are the stator leakage, rotor leakage and mutual inductances, respectively. In order for the rotor mmf to be in synchronism with the stator mmf, the frequency of the rotor current, ω_{rf}, must satisfy the slip frequency constraint

$$\omega_{rf} = \omega_s - \omega_r = s\omega_s \quad (19)$$

The per-unit electromagnetic torque equation is given by

$$T_e = \lambda_{ds} i_{qs} - \lambda_{qs} i_{ds} = \lambda_{qr} i_{dr} - \lambda_{dr} i_{qr} = L_m(i_{qs} i_{dr} - i_{ds} i_{qr}) \quad (20)$$

Neglecting the power losses associated with the stator and rotor resistances, the active and reactive stator powers are:

$$P_s = \tfrac{3}{2}(v_{ds} i_{ds} + v_{qs} i_{qs}) \quad (21)$$

$$Q_s = \tfrac{3}{2}(v_{qs} i_{ds} - v_{ds} i_{qs}) \quad (22)$$

and the active and reactive rotor powers are given by

$$P_r = \tfrac{3}{2}(v_{dr} i_{dr} + v_{qr} i_{qr}) \quad (23)$$

$$Q_r = \tfrac{3}{2}(v_{qr} i_{dr} - v_{dr} i_{qr}) \quad (24)$$

E) Matlab/Simulink Model of Wound Round Induction Generator and Back-To Back IGBT Converters

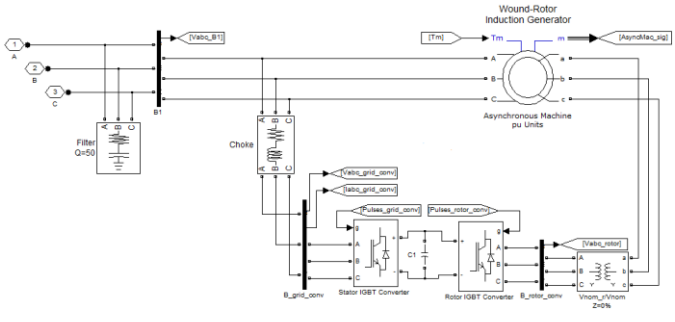

Figure 4 Matlab/Simulink Model of Wound Round Induction Generator and Back-To Back IGBT Converters

III) DESIGN OF THE CONTROL SYSTEM

The objective of the RSC is to govern both the stator-side active and reactive powers independently; while the objective of the GSC is to keep the dc-link voltage constant regardless of the magnitude and direction of the rotor power. The GSC control scheme can also be designed to regulate the reactive power. The wind turbine controller controls the pitch angle of the blades, which determine the mechanical power that the turbine extracts from the wind.[5] [6].

A) Design of the RSC Controllers

in stator-flux oriented reference frame the *d*-axis is aligned with the stator flux linkage vector λ_s, namely, $\lambda_{ds} = \lambda_s$ and $\lambda_{qs} = 0$. This gives the following relationships

$$i_{qs} = -L_m i_{qr} / L_s \quad (25)$$

$$i_{ds} = L_m(i_{ms} - i_{dr}) / L_s \quad (26)$$

$$P_s = -\tfrac{3}{2}\omega_s L_m^2 i_{ms} i_{qr} / L_s \quad (27)$$

$$Q_s = \tfrac{3}{2}\omega_s L_m^2 i_{ms}(i_{ms} - i_{dr}) / L_s \quad (28)$$

$$v_{dr} = r_r i_{dr} + \sigma L_r p i_{dr} - s\omega_s \sigma L_r i_{qr} \quad (29)$$

$$v_{qr} = r_r i_{qr} + \sigma L_r p i_{qr} + s\omega_s\left(\sigma L_r i_{dr} + L_m^2 i_{ms} / L_s\right) \quad (30)$$

Equations (28) and (29) indicate that P_s and Q_s can be controlled independently by regulating the rotor current components, i_{qr} and i_{dr}, respectively. Consequently, the reference values of i_{dr} and i_{qr} can be determined from the outer power control loops. [3] [13]

B) Design of the Inner Current Control Loops in

Let

$$v_{dr1} = r_r i_{dr} + \sigma L_r p i_{dr} \quad (31)$$

$$v_{qr1} = r_r i_{qr} + \sigma L_r p i_{qr} \quad (32)$$

representing parts of (30) and (31), then (34) and (35) can be rewritten into a matrix form as

$$p\begin{bmatrix} i_{dr} \\ i_{qr} \end{bmatrix} = -\frac{r_r}{\sigma L_r}\begin{bmatrix} 1 & 0 \\ 0 & 1 \end{bmatrix} i_{dr} + \frac{1}{\sigma L_r}\begin{bmatrix} v_{dr1} \\ v_{qr1} \end{bmatrix} \quad (33)$$

Equation (33) indicates that i_{dr} and i_{qr} respond to v_{dr1} and v_{qr1} respectively, through a first-order transfer function without cross-coupling. It is therefore possible to design the following feedback loops and PI controllers

$$v_{dr1} = \left(k_{pr} + \frac{k_{ir}}{s}\right)(i_{dr}^* - i_{dr}) \quad (34)$$

$$v_{qr1} = \left(k_{pr} + \frac{k_{ir}}{s}\right)(i_{qr}^* - i_{qr}) \quad (35)$$

Substituting (34) and (35) into (29) and (28) gives

$$v_{dr} = \left(k_{pr} + \frac{k_{ir}}{s}\right)(i_{dr}^* - i_{dr}) - s\omega_s \sigma L_r i_{qr} \quad (36)$$

$$v_{qr} = \left(k_{pr} + \frac{k_{ir}}{s}\right)(i_{qr}^* - i_{qr}) + s\omega_s\left(\sigma L_r i_{dr} + \frac{L_m^2}{L_s} i_{ms}\right) \quad (37)$$

C) Design of the Speed Controller:

The shaft system model has a significant impact on the dynamic behaviour of the WTG and the design of the speed controller. In terms of the transfer function from the EM torque, T_e, to rotor speed, ω_r, for the two-mass shaft system (with $D_t = D_g = 0$) is given by

$$\frac{\omega_r}{T_e} = \frac{1}{2(H_t + H_g)} \frac{1}{s} \frac{2H_t s^2 + D_{tg} s + K_{tg}}{\frac{2H_t H_g}{H_t + H_g} s^2 + D_{tg} s + K_{tg}} \quad (38)$$

which can be viewed as a lumped-mass system, $1/[2(H_t+H_g)s]$, The frequencies of the torsional oscillation modes are given by:

$$\omega_1 = \sqrt{\frac{K_{tg}}{2H_t}}, \quad \omega_2 = \sqrt{\frac{K_{tg}}{2H_t H_g/(H_t + H_g)}} \quad (39)$$

In order to improve the damping of the low-frequency torsional oscillations of the two-mass system, the speed controller has to be designed so that the closed-loop system has a sufficiently low bandwidth less than ω_1. For the lumped-mass model, the transfer function from T_e to ω_m, according to (with $D_m = 0$), is given by

$$\frac{\omega_m}{T_e} = \frac{1}{2H_m s} \quad (40)$$

which is the same as the lumped-mass part in . In such a model, there are no low-frequency oscillating components, and the speed controller therefore can be designed with a higher bandwidth. However, the lumped-mass model might be insufficient to represent the dynamic behaviour of the WTG system.

Fig. [5] shows the overall vector control scheme of the RSC.

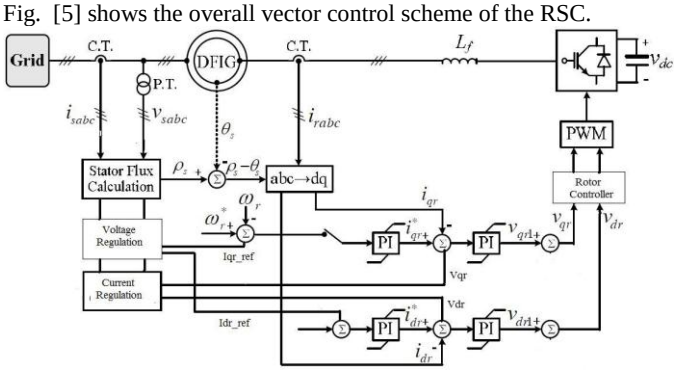

Figure 5. Overall vector control scheme of the RSC.

D) Matlab/Simulink Design of Rotor Side Controller

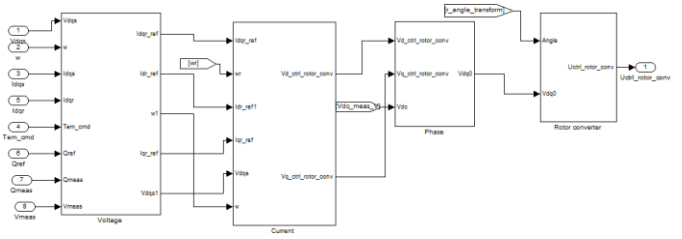

Figure 6 Matlab/Simulink Design of Rotor Side Controller

E) Design of the GSC Controllers

The GSC control scheme also consists of two cascaded control loops. The inner current control loops regulate independently the *d*-axis and *q*-axis GSC ac-side current components, i_{dg} and i_{qg}, in the synchronously rotating reference frame. The outer control loops regulate the dc-link voltage and the reactive power exchanged between the GSC and the grid.

Ac-side circuit equations of the GSC can be written as

$$p i_{gabc} = -\frac{r_g}{L_g} i_{gabc} + \frac{1}{L_g}(v_{gabc} - v_{sabc}) \quad (41)$$

Applying the synchronously rotating reference frame transformation to with the *d*-axis aligned to the grid voltage vector v_s ($v_s = v_{ds}$, $v_{qs} = 0$), the following *d-q* vector representation can be obtained for modeling the GSC ac-side. [3]

$$v_{dg} = r_g i_{dg} + L_g p i_{dg} - \omega_s L_g i_{qg} + v_s \quad (42)$$

$$v_{qg} = r_g i_{qg} + L_g p i_{qg} + \omega_s L_g i_{dg} \quad (43)$$

Following the same procedure as in (31)-(37), v_{dg} and v_{qg} can be obtained by the following feedback loops and PI controllers

$$v_{dg} = \left(k_{pg} + \frac{k_{ig}}{s}\right)(i_{dg}^* - i_{dg}) - \omega_s L_g i_{qg} + v_s \quad (44)$$

$$v_{qg} = \left(k_{pg} + \frac{k_{ig}}{s}\right)(i_{qg}^* - i_{qg}) + \omega_s L_g i_{dg} \quad (45)$$

where the reference values i_{dg} * and i_{qg} * are obtained from the outer control loop.

F) Design of the Dc-link Voltage Controller:

Neglecting harmonics due to switching and the losses in the GSC, the filtering inductor and the transformer the power balance equation is given by

$$P_r - P_g = v_{dc} i_{dc} = C v_{dc} p v_{dc} \quad (46)$$

Let

$$v_{dc} = v_{dc0} + \Delta v_{dc} \quad (47)$$

where v_{dc0} (= v_{dc} *) is the dc component of v_{dc}, Δv_{dc} is the ripple component of v_{dc}. Substituting (46) into (47) gives

$$P_r - P_g = C v_{dc0} p v_{dc} + C \Delta v_{dc} p v_{dc} \quad (48)$$

Since $\Delta v_{dc} << v_{dc}0$, (48) can be written as

$$P_r - P_g \approx C v_{dc0} p v_{dc} \quad (49)$$

Therefore, the transfer function from Pg to v_{dc} is given by

$$\frac{v_{dc}(s)}{P_g(s)} = \frac{1}{C v_{dc0} s} \quad (50)$$

Since

$$P_g = \frac{3}{2} v_{ds} i_{dg} = \frac{3}{2} v_s i_{dg} \quad (51)$$

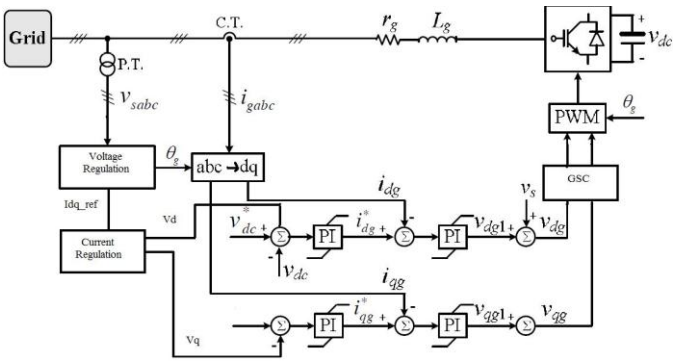

Figure 7 Overall vector control scheme of the GSC

(eq. 50) becomes

$$\frac{v_{dc}(s)}{i_{dg}(s)} = \frac{\frac{3}{2}v_s}{Cv_{dc0}s} \qquad (52)$$

Therefore, it is possible to design a feedback loop and PI controller to generate the reference value of i_{da} as follows

$$i_{dg}^{*} = \left(k_{pv} + \frac{k_{iv}}{s}\right)(v_{dc}^{*} - v_{dc}) \qquad (53)$$

G) Matlab Implementation of GSC

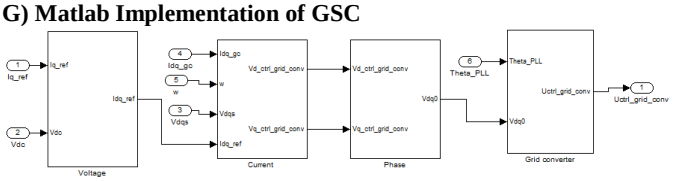

Figure 8 Matlab Implementation Of GSC

H) Reactive Power Control:

The reactive power exchanged between the GSC and the grid is given by

$$Q_g = -\frac{3}{2}v_{ds}i_{qg} = -\frac{3}{2}v_s i_{qg} \qquad (54)$$

Therefore, the reference value of i_{dg} can be determined directly from the reactive power command.

IV) DESIGN OF THE PITCH ANGLE (β) CONTROLLER

The pitch angle controller is only activated at high wind speeds. Fig. 9 shows the structure of the pitch angle controller. P_e is the total output active power from the DFIG.

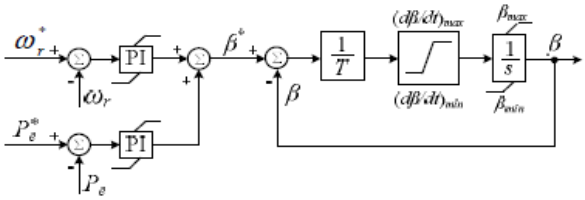

Figure 9 Wind turbine pitch angle controller.

V. RESULT & DISCUSSION

Case IV) DFIG operation under grid fault condition

In the following simulation, the fault is applied during sub synchronous operation. Before the fault takes place, the DFIG operates at the rotor speed of 0.83 pu. The generator produces active power of 9M.w and the reactive power is set at neutral. The voltage terminal before the fault is around 1 pu. The responses of the DFIG during the simulation are presented.

When generator disconnection is not ordered, the rotor speed accelerates abruptly towards synchronous speed after the converter is blocked. At this instant, the generator is situated in a motoring operation. As can be seen in the results, the generator absorbs a large amount of active power until it comes into to a generating operation again, when the rotor speed arrives at around 2% above the synchronous speed.

A sudden change of the rotor speed results in shaft oscillation. This oscillation induces fluctuation in the active and reactive power. Further, these fluctuations prolong the recovery of the terminal voltage after fault clearance.

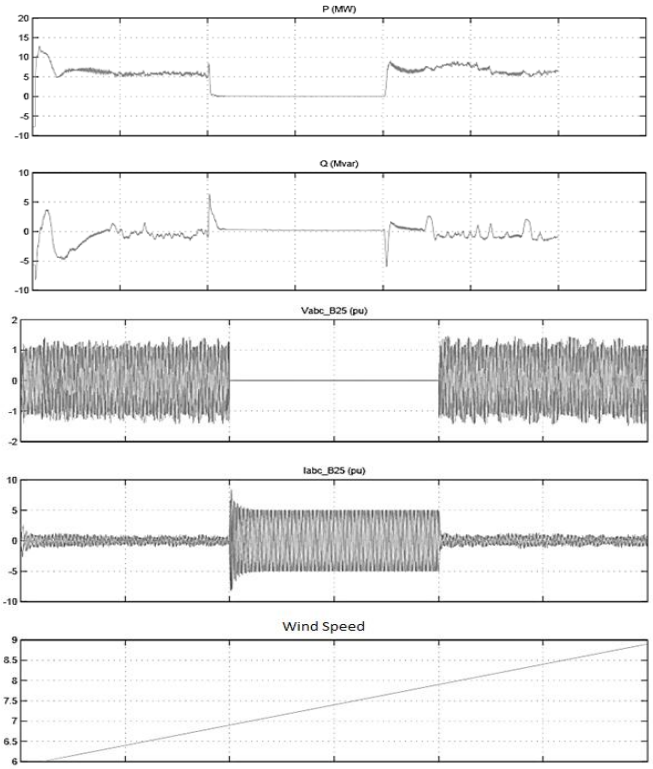

Figure 13. DFIG operation under grid fault condition

Case VII) DFIG response to phase faults in super synchronous speed

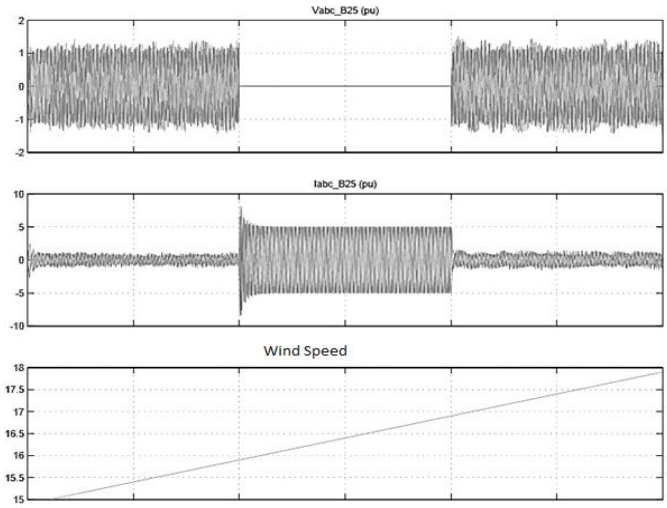

Figure 16. DFIG response to phase faults in super synchronous speed

Initially the generator operates at super-synchronous speed where the rotor speed is 1.02 pu. At this moment, the DFIG generates the active power of 9 M.W while the reactive power is set at zero.

The fault is applied at t = 1.s for 1 min duration with a short circuit resistance of 0.016 pu. The fault causes the terminal voltage to drop to approximately 0.2 pu. Subsequently, the following sequence takes place.

If the generator is allowed to remain connected to the grid, it tends to absorb a large amount of reactive power, while in the meantime the

stator current and the active power fluctuate, particularly after the fault is cleared. The absorption of a large amount of the reactive power may induce instability on the line, especially for large-scale wind parks.

VI CONCLUSION

This paper presents a study of the dynamic performance of variable speed DFIG coupled with wind turbine and the power system is subjected to disturbances; such as voltage sag, unbalanced operation or short circuit faults. The dynamic behaviour of DFIG under power system disturbance was simulated MATLAB/SIMULINK platform using d-q vector control concept. Accurate transient simulations are required to investigate the influence of the wind power on the power system stability.

In the present investigation, the dynamic DFIG performance is presented for both normal and abnormal grid conditions. The control performance of DFIG is satisfactory in normal grid conditions and it is found that, both active and reactive power maintains a steady pattern in spite of fluctuating wind speed and net electrical power supplied to grid is maintained constant. During grid disturbance, considerable torque pulsation of DFIG and torsional oscillation in drive train system has been observed.

It is also observed that the dynamic behaviour of DFIG under sub synchronous speed needs special attention than when it operates in super synchronous speed.

As regards the saturation effect during fault, is not considered as it has direct impact on the peak value of the stator and rotor current under fault condition.

Therefore it is important to take the saturation effect into account, especially when designing a protection setting.

Further models for the DFIG were developed by adding the behaviour of converters. These converters allow the DFIG to be controlled to not only perform the basic functions of a variable speed wind turbine, but also to improve power system performance. We derived two generic control strategies and showed how they affected the performance of a DFIG. Understanding of the effects of faults and protection systems on DFIGs was increased by observing the model behaviour.

APPENDIX

The parameters of the simulated DFIG are shown in Table I

Table I [15]

Rated Power	6 X 1.5 = 9 MW
Stator frequency	60 Hz
Stator nominal voltage	575 V
Stator resistance	0.023 pu
Stator Inductance	0.18 pu
rotor resistance	0.016 pu
rotor Inductance	0.16 pu
Inertia constant	0.685 pu
Nominal DC bus voltage	1150 V

REFERENCE

[1] A. Perdana, O. Carlson, and J. Persson, *"Dynamic Response of Grid-Connected WindTurbine with Doubly Fed Induction Generator during Disturbances",* Nordic Workshop On Power And Industrial Electronics. Trondheim – 2004

[2] B.Chitti Babu , K.B.Mohanty *"Doubly-Fed Induction Generator for Variable Speed Wind Energy Conversion Systems- Modeling & Simulation"* International Journal of Computer and Electrical Engineering, Vol. 2, No. 1, February, 2010 1793-8163 : -

[3] Miguel Castilla, Jaume Miret, *Member* IEEE, *"Direct Rotor Current-Mode Control Improves the Transient Response of Doubly Fed Induction Generator-Based Wind Turbines"* IEEE TRANSACTIONS ON ENERGY CONVERSION, VOL. 25, NO. 3, SEPTEMBER 2010

[4] P. S. Mayurappriyan 1, Jovitha Jerome 2, *"Dynamic Modeling and Analysis of Wind Turbine Driven Doubly Fed Induction Generator"* International Journal of Recent Trends in Engineering, Vol 2, No. 5, November 2009

[5] Jiaqi Liang, *Student Member, IEEE* Wei Qiao, *Member, IEEE*, and Ronald G. Harley, *Fellow, IEEE* "*Feed-Forward Transient Current Control for Low-Voltage Ride-Through Enhancement of DFIG Wind Turbines*" IEEE TRANSACTIONS ON ENERGY CONVERSION, VOL. 25, NO. 3, SEPTEMBER 2010

[6] Yi Zhou, *Student Member, IEEE*, Paul Bauer, *Senior Member, IEEE "Operation of Grid-Connected DFIG Under Unbalanced Grid Voltage Condition"* IEEE TRANSACTIONS ON ENERGY CONVERSION, VOL. 24, NO. 1, MARCH 2009

[7] Balasubramaniam Babypriya — Rajapalan Anita *"Modelling, Simulation And Analysis Of Doubly Fed Induction Generator For Wind Turbines"* Journal of ELECTRICAL ENGINEERING, VOL. 60, NO. 2, 2009, 79–85

[8] Jing Zhao, Wei Zhang, Yikang He, Jiabing Hu *"Modeling and Control of a Wind-Turbine-Driven DFIG Incorporating Core Saturation During Grid Voltage Dips"* , College of Electrical Engineering, Zhejiang University, Hangzhou, China

[9] Xiangwu Yan, *Member, IEEE*, Giri Venkataramanan, *Senior Member, IEEE, "Voltage-Sag Tolerance of DFIG Wind Turbine With a Series Grid Side Passive-Impedance Network*" ,IEEE TRANSACTIONS ON ENERGY CONVERSION, VOL. 25, NO. 4, DECEMBER 2010

[10] Jiabing Hu, *Member, IEEE*, Heng Nian, *Member, IEEE*, Bin Hu, Yikang He, *Senior Member, IEEE*, *"Direct Active and Reactive Power Regulation of DFIG Using Sliding-Mode Control Approach"* IEEE Transactions On Energy Conversion, Vol. 25, No. 4, December 2010

[11] Ana I. Estanqueiro, *Member, IEEE "A Dynamic Wind Generation Model for Power Systems Studies"*, IEEE Transactions On Power Systems, Vol. 22, No. 3, August 2007

[12] Bimal K Bose Condra Chair Excellence in power electronics, University of Tennessee, "*A Book on Modern Power Electronics and AC Drives"* Pearson Education Ltd. ISBN : 0-13-016743-6

[13] Ake Larson, "*Thesis for the degree of doctorate of philosophy on the power quality of wind turbines"* Department of Electric power engineering, Chalmers University of Technology, Sweeden 2000, ISBN : 91-7197-970-0.

[14] Wei Qiao" Dynamic Modeling and Control of Doubly Fed Induction Generators Driven by Wind Turbines "IEEE/PES Power Systems Conference and Exposition, 2009. PSCE '09. Digital Object Identifier: 10.1109/PSCE.2009.4840245

[15] ANDREAS PETERSSON "*Analysis, Modeling and Control of Doubly-Fed Induction Generators for Wind Turbines"* Division of Electric Power Engineering Department of Energy and Environment CHALMERS UNIVERSITY OF TECHNOLOGY G¨oteborg, Sweden 2005 , ISBN 91-7291-600-1

*1. **Ram Mohana Vamsee.B***, M.Tech Student in Electrical Power Systems, Bharati Vidyapeeth Deemed University College of Engineering Pune

*2. **Prof. D. S .Bankar***, Ph.D. candidate at Bharati Vidyapeeth University, Currently working as Associate Professor in Electrical Engineering Department of Bharati Vidyapeeth University College of Engineering Pune, India

3. ***Dr D. B. Talange***, Ph.D IIT Bombay, Specialization in Systems and Control Engineering, currently working as Professor in Electrical Engineering Department of Govt. College of Engineering Pune-411 005 (India)